Journal of Pharmaceutical Investigation
https://doi.org/10.1007/s40005-020-00472-1

Online ISSN 2093-6214
Print ISSN 2093-5552

ORIGINAL ARTICLE

In vitro and in vivo evaluation of a novel nitric oxide-releasing ointment for the treatment of methicillin-resistant *Staphylococcus aureus*-infected wounds

Juho Lee[1] · Shwe Phyu Hlaing[1] · Jiafu Cao[1] · Nurhasni Hasan[1] · Jin-Wook Yoo[1]

Received: 26 November 2019 / Accepted: 5 February 2020

Abstract

Purpose Nitric oxide (NO) has emerged as a novel agent for the treatment of infected wounds owing to its potent wound-healing effects and antibacterial activity against drug-resistant bacteria, including methicillin-resistant *Staphylococcus aureus* (MRSA). In this study, we developed a NO-releasing ointment composed of S-nitrosoglutathione (GSNO) and polyethylene glycol (PEG) for the treatment of MRSA-infected cutaneous wounds.

Methods The GSNO-incorporated PEG ointment (GPO) was successfully prepared by homogeneous dispersion of micronized GSNO in a PEG ointment base. High encapsulation efficiency was achieved (97.25%) via water-free fabrication processing of the GPO, resulting in minimal GSNO hydrolysis.

Results When applied to a wound, the wound fluid triggered the degradation of GSNO and NO was released from the GPO for 24 h without an initial burst release. The GPO exhibited potent antibacterial effects against MRSA without cytotoxic effects against L929 cells. An in vivo wound healing experiment using a mouse MRSA-challenged full-thickness wound model revealed that the GPO could facilitate healing of infected wounds.

Conclusion Thus, the GPO could be a promising NO-releasing formulation for the treatment of infected cutaneous wounds.

Keywords Nitric oxide · S-nitrosoglutathione · Methicillin-resistant *staphylococcus aureus* · Infected wound healing · Ointment

Introduction

Cutaneous wound infections remain a global problem, and their treatment costs millions of dollars per year (Daeschlein 2013). In addition, wound infections can cause severe complications, including sepsis, the mortality due to which is greater than 30% in the United States (Fleischmann et al. 2016). Wound healing occurs spontaneously through three sequential phases: inflammation, cell proliferation, and tissue remodeling (Bello and Phillips 2000; Witte and Barbul 1997); however, wounds are frequently contaminated by various bacteria that induce continuous inflammation at the wound site (Yurt et al. 1984). Due to the chronic inflammation caused by the bacteria, the healing process of an infected wound is stalled at the inflammatory phase, resulting in delayed wound healing. For these reasons, eradication of bacteria from the wound is essential for successful treatment (Choi et al. 2019).

For the treatment of infected wound, antibacterial ointments are widely used for the treatment of infected wounds as these are easily applied to bendable areas of the human body and require less costly manufacturing compared with other wound dressings such as bandages and films. For these reasons, various antibacterial ointments are commercially available. However, wound infections caused by antibiotic-resistant bacteria, including methicillin-resistant *Staphylococcus aureus* (MRSA), have emerged as a severe problem in infected wound treatment (Rosen et al. 2016). In addition to delayed wound healing, MRSA can invade the systemic circulation and cause life-threatening complications, including sepsis (Daeschlein 2013; Fleischmann et al. 2016). Therefore, the development of novel antibacterial ointments for the treatment of infected wounds (especially MRSA infection) is urgently required (Hasan et al. 2019a).

✉ Jin-Wook Yoo
jinwook@pusan.ac.kr

[1] College of Pharmacy, Pusan National University, Busan 609-735, South Korea

Published online: 13 February 2020

As a novel wound healing agent, nitric oxide (NO) has gained much attention in recent years due to its beneficial promotion of angiogenesis, cell proliferation, and tissue remodeling (Bogdan 2001; Schäffer et al. 1996; Wallace 2005). In addition, NO possesses broad-spectrum antibacterial activity, elicited via the formation of reactive oxidative and nitrosative species, which can damage bacterial cell membranes, proteins, and bacterial DNA (Hasan et al. 2019b; Jones et al. 2010). These multiple antibacterial mechanisms can inhibit the emergence of NO-resistant bacteria, whereas current antibiotics are susceptible to antibiotic resistance (Jones et al. 2010; Privett et al. 2012; Stratton 2003). Moreover, due to its various bactericidal mechanisms, NO exerts antibacterial effects against drug-resistant bacteria, including MRSA (Schairer et al. 2012). Thus, NO could be an ideal agent for the treatment of infected wounds due to its beneficial effects on skin cell proliferation and tissue remodeling as well as its potent antibacterial effects. However, although NO possesses various beneficial properties for accelerating wound healing, application of NO as a therapeutic agent is challenging due to its volatile, short-lived nature (Nurhasni et al. 2015). In addition to gaseous NO, solid-state NO-releasing molecules (NO donors), such as diazeniumdiolates and S-nitrosothiols, are readily degraded by hydrolysis. Moreover, the low solubility of NO donors in organic solvents has been a hurdle in the fabrication of homogeneous formulations.

In this study, we developed an NO-releasing ointment consisting of S-nitrosoglutathione (GSNO) and polyethylene glycol (PEG): an endogenous NO donor and a widely used biocompatible ointment base, respectively. GSNO is a widely used NO donor and active pharmaceutical ingredient of NO-releasing wound dressings, such as hydrogels, films, and microparticulate systems (Amadeu et al. 2007; Georgii et al. 2011; Hlaing et al. 2018; Kim et al. 2015; Schanuel et al. 2015). PEG, a highly biocompatible hydrophilic polymer, was used as an ointment base to obtain a homogeneously dispersed GSNO ointment. After the preparation and characterization of the GSNO-incorporated PEG ointment (GPO), the in vitro antibacterial effect was evaluated using a LIVE/DEAD® *Bac*Light™ bacterial viability kit against MRSA, a representative antibiotic-resistant bacterium. The in vivo facilitated wound healing efficacy of the GPO was evaluated using a mouse MRSA-challenged full-thickness wound model.

Materials and methods

Materials

Glutathione (reduced-form) was purchased from Wako Pure Chemical (Osaka, Japan). Polyethylene glycol (PEG) 200 (average molecular weight: 200) and PEG 4000 (average molecular weight: 4000) were purchased from Yakuri Co., Ltd. (Osaka Japan). Sodium nitrite, 2,2,2 tribromoethanol, tert-amyl alcohol, Mayer's hematoxylin, eosin-Y disodium, thiazolyl blue tetrazolium bromide (MTT) were purchased from Sigma-Aldrich (St. Louis, MO). Bacto™ tryptic soy broth (TSB) and Difco™ cetrimide-agar media were purchased from BD Biosciences (San Jose, CA, USA). A LIVE/DEAD® *Bac*Light™ bacterial viability kit was purchased from Thermo Fisher Scientific (Waltham, MA, USA). Dulbecco's modified Eagle's media (DMEM), fetal bovine serum (FBS), and penicillin–streptomycin were purchased from Hyclone (Thermo Fisher Scientific Inc., MA, USA). All other materials and solvents used were of the highest analytical grade.

Synthesis of GSNO

GSNO was synthesized from GSH and acidified nitrite, as previously described with some modifications (Broniowska et al. 2013; Parent et al. 2013). Briefly, sodium nitrite and GSH were introduced into an ice-cold hydrochloric acid (HCl) solution and stirred for 40 min (final concentrations of sodium nitrite, GSH, and HCl were 0.625 M). To precipitate GSNO, acetone was added to the solution. The precipitate was collected and washed twice using acetone and thrice using diethyl ether. After washing, GSNO was vacuum-dried and stored at − 20 °C in a refrigerator until use.

Preparation and characterization of the GSNO-incorporated PEG ointment

The GSNO-incorporated PEG ointment (GPO) was prepared with GSNO, PEG 4000, and PEG 200. The GPO was fabricated in a two-step process: fabrication of homogeneous GSNO-PEG suspension and a sol–gel transition step by cooling. Briefly, 0.125 g GSNO was dispersed in 2 g PEG 200 and sonicated. When GSNO was homogeneously suspended in PEG 200, the GSNO-PEG 200 suspension was mixed with 1 g preheated PEG 4000 (70 °C). After blending, the liquid GPO was cooled to room temperature (around 20 °C) with continuous stirring. The GPO was stored in a dry place away from light. Blank PEG ointment (PO) was prepared by the same method except for the addition of GSNO. The homogeneity of the GPO and GSNO content were analyzed using a UV–Vis spectrophotometer (U-5100, Hitachi, Tokyo, Japan).

NO release measurements

NO release from the GPO was evaluated using previously described methods with some modification (Lee et al. 2019). Briefly, 40 mg GPO was placed at the bottom of

a 2 mL-microtube; 700 µL simulated wound fluid (SWF) (Homsy 1970; Lin et al. 2001) was added to the GPO and incubated in an incubator at 37 °C. The SWF consisted of 0.64% NaCl, 0.22% KCl, 2.5% $NaHCO_3$, and 0.35% NaH_2PO_4 in distilled water (DW), with a pH adjusted to 7.4. At each time point, the amount of remaining GSNO in the GPO was measured using a UV/vis spectrophotometer at a wavelength of 335 nm. NO released from the GPO at each time point ($[NO]_t$) was calculated using a previously reported equation: ($[GSNO]_0$: initial GSNO concentration, $[GSNO]_t$: GSNO concentration at each time point) (Yoo et al. 2009).

$$[NO]_t = [GSNO]_0 - [GSNO]_t$$

Antibacterial activity

The antibacterial activity of the GPO against MRSA was investigated using a LIVE/DEAD® *Bac*Light™ bacterial viability kit. MRSA was incubated overnight in TSB media before drug treatment. MRSA was washed twice with normal saline and added to the GPO and incubated at 37 °C. After 24 h, the MRSA was washed and stained according to the manufacturer's instructions. Stained MRSA was observed under a confocal laser fluorescence microscope (Fluoview FV10i, Olympus, Tokyo, Japan) at a magnification of × 100. The excitation/emission (Ex/Em) wavelengths for SYTO 9 and propidium iodide (PI) were 480/500 nm and 490/635 nm, respectively. Green fluorescence in the resulting images was measured using ImageJ software (National Institutes of Health, Bethesda, MA, USA) for the quantification of live bacteria.

Cytotoxicity testing

Cytotoxicity of the GPO was evaluated against L929 murine fibroblasts using the MTT assay. Briefly, L929 cells were purchased from the Korean Cell Line Bank (KCLB, Seoul, Korea) and grown in DMEM containing 10% FBS and 1% penicillin/streptomycin in 5% CO_2 at 37 °C. For the MTT assay, cells were seeded in 96-well plates at a density of 20,000 cells per well. After overnight incubation, different concentrations of the GPO were added and incubated for 24 h. Then, the media were replaced with 1 mg/mL of MTT solution. Two hours later, 100 µL DMSO was added to each well after the removal of the supernatant. After the resulting formazan crystals were dissolved, the absorbance of each well was measured at 540 nm using a microplate reader (iMark Microplate Reader, Bio-Rad Laboratories Inc., Richmond, CA).

In vivo wound healing study

All animal experiments were reviewed and approved by the Pusan National University Institutional Animal Care and Use Committee (PNU-IACUC) on 01 February 2018 (PNU-2018-1800). The therapeutic activity of the GPO against MRSA-infected wounds was evaluated in a mouse MRSA-challenged full-thickness wound model (Lee et al. 2019). Briefly, male ICR mice (6 weeks old) were purchased from Samtako Bio (Osan, Korea) and allowed to acclimatize for 1 week. To create an MRSA-challenged full-thickness wound, mice were anesthetized with 0.5 mg/g of 2,2,2 tribromoethanol (Avertin). After the induction of anesthesia, the dorsal area was shaved using an electric razor and hair removal cream (Veet for sensitive skin, Reckitt Benckiser, France). A full-thickness wound was created using an 8-mm biopsy punch; subsequently, 10^8 CFUs of MRSA were challenged to the wound. Each wound was covered with a Tegaderm film for 24 h to induce infection. On the following day, mice were randomly arranged into three groups: GPO-treated, PO-treated, and untreated groups. After imaging the wounds, approximately 40 mg GPO was applied to each wound. Imaging wound site and drug treatment were performed every 2 days. The wound size was determined using ImageJ software. For histological analysis, mice were euthanized, and each wound was excised using an 8-mm biopsy punch 10 days after treatment initiation. Collected wound samples were fixed and embedded in paraffin blocks and sectioned. Five-micrometer sections of each wound were stained with hematoxylin and eosin (H&E) according to the manufacturer's protocol. After staining, samples were observed at a magnification of × 20 using light microscopy.

Statistical analysis

All data were expressed as the mean ± SD. Statistical analyses were performed using two-way ANOVA and one-way ANOVA, followed by Bonferroni's test using GraphPad Prism 5.0 software (GraphPad Software, Inc., La Jolla, CA). P values < 0.05 were considered statistically significant.

Results and discussion

Preparation and characterization of the GPO

The GPO was successfully prepared by incorporating GSNO into a PEG ointment base using melting-homogenizing and cooling processes (Fig. 1a). Due to the high hydrophilicity of GSNO, GSNO powders could be more easily dispersed in liquid PEG than in other ointment bases, including petroleum jelly, which is a highly lipophilic ointment base. As micronized GSNO particles were evenly dispersed

in PEG, the GPO was a light pink-colored semi-solid ointment (Fig. 1b). In addition, large GSNO particles were not observed under macroscopic examination. To evaluate content homogeneity and GSNO loading in the GPO, the GSNO concentration was measured in 10 different GPO samples. As GSNO has a characteristic absorption peak at a wavelength of 335 nm, (extinction coefficient: 922 M^{-1} cm^{-1}) (Broniowska et al. 2013; Hornyák et al. 2011), the absorption peak at a wavelength of 335 nm was measured by UV/Vis spectrophotometry; the concentration of GSNO was calculated using the Beer-Lambert equation. As shown in Fig. 1c, the GPO exhibited homogenous GSNO content with a narrow standard deviation. GSNO loading of the GPO was 3.89 ± 0.09%; the encapsulation efficacy was 97.25%. The GSNO content of the GPO was designed to achieve a target concentration of 4% of the total weight, as previously reported GSNO formulations that demonstrated in vivo therapeutic efficacy had concentrations of 3 to 5% (Amadeu et al. 2007; Hlaing et al. 2018; Lee et al. 2019). Degradation of GSNO was minimized due to the water-free fabrication process, resulting in high encapsulation efficacy of the GPO. Moreover, GSNO decomposition during storage may be minimized, which ensures high storage stability of the GPO under light shielding and well-sealed conditions.

NO release measurements

To investigate the NO release profile of the GPO, NO release was measured by detecting the decomposition of GSNO (as 1 mol of NO can be released from 1 mol of GSNO by hydrolysis). When exposed to SWF, NO liberation is triggered along with the dissolution and hydrolysis of GSNO in the GPO. The GPO exhibited sustained NO release within 24 h without burst release (Fig. 2), indicating that the GPO could exert antibacterial and wound healing promotion for 24 h after application. As the polymeric structure of PEG could restrict diffusion of GSNO and NO molecules, the release of NO from the GPO was more prolonged than that from a GSNO solution (< 12 h, data not shown). Delayed NO release was observed in the

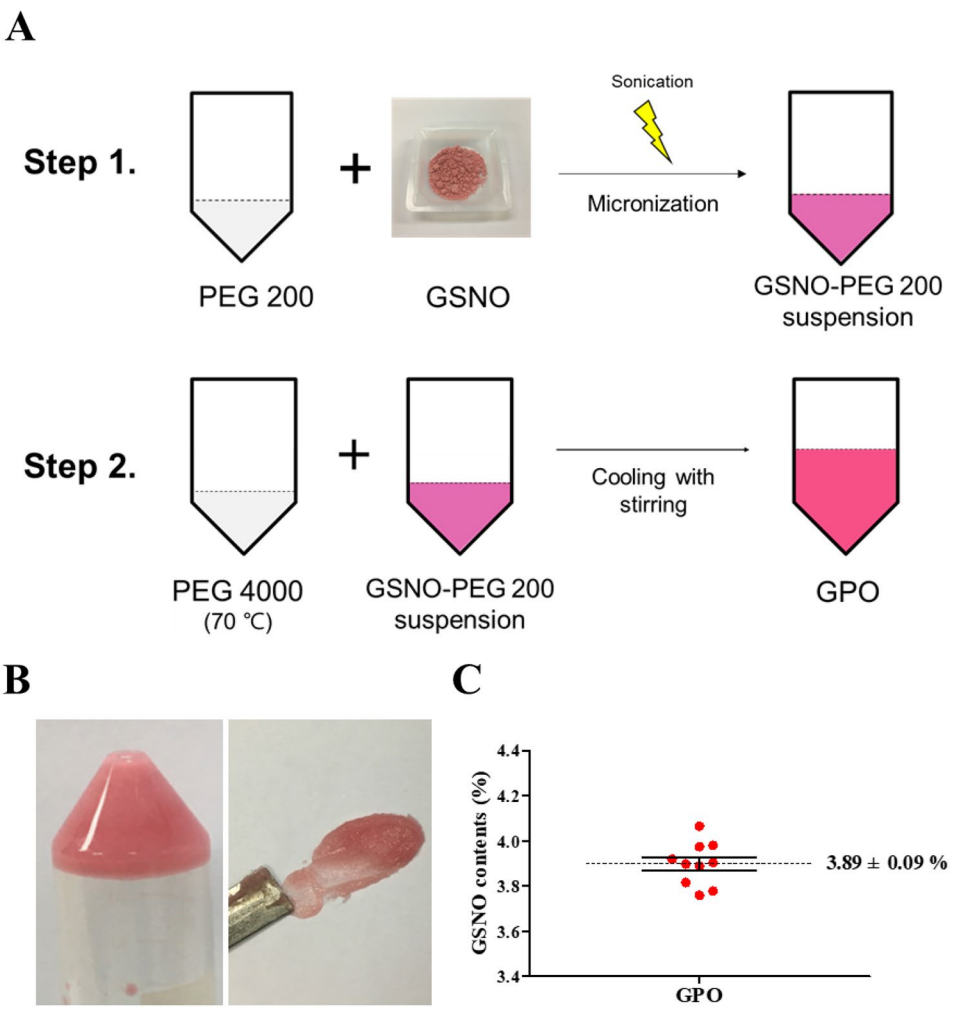

Fig. 1 **a** Schematic description of GSNO-incorporated PEG ointment (GPO) preparation. **b** Macroscopic images of the GPO. **c** GSNO contents of GPO. Data were expressed as mean ± standard deviation (n = 10)

first 2 h as NO release was probably initiated after the dissolution of GSNO. In addition, as the GPO exhibited continuous NO release without the burst release phenomena, the applied GPO could be converted to new GPO anytime within 24 h. This ability may increase the convenience in the use of the GPO for patients who are uncomfortable with frequent dressing changes. Moreover, as the color of the GPO changes from pink to ivory during GSNO decomposition, patients can readily determine when the ointment needs to be changed by observing the color of the GPO.

Antibacterial activity

The antibacterial activity of the GPO against MRSA was studied using the LIVE/DEAD® *Bac*Light™ bacterial viability kit. SYTO 9 (green fluorescence) can penetrate all bacterial membranes whereas PI (red fluorescence) is impermeable to live bacteria. When the bacterial membrane is damaged, PI can be internalized and stains bacterial DNA in place of SYTO 9. Therefore, live and dead bacteria exhibit green fluorescence or red fluorescence, respectively. As shown in Fig. 3a, images of untreated and PO-treated groups exhibited a large amount of green fluorescence whereas the GPO exhibited low levels of green fluorescence. As the MRSA in the GPO-treated group could be damaged by the NO released from the GPO, the viability of MRSA incubated with the GPO was significantly decreased compared to the PO-treated and untreated groups (Fig. 3b). Although MRSA exhibits antibiotic resistance to various antibiotic agents, the GPO exhibited potent bactericidal effects against MRSA owing to the multiple NO bactericidal mechanisms that provide broad-spectrum antibacterial effects that are highly effective against drug-resistant bacteria and suppress the emergence of NO-resistant bacteria.

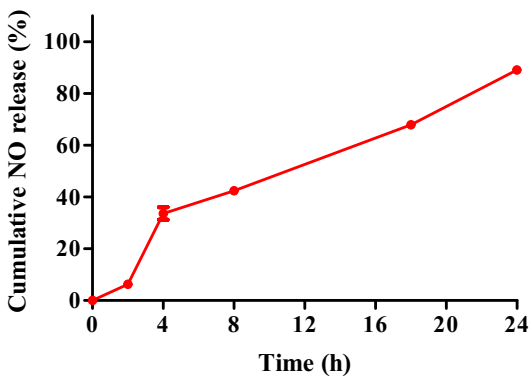

Fig. 2 NO release profile of the GPO. Results are presented as the mean ± SD (n = 3)

Cytotoxicity test

To evaluate the cytotoxic effect of the GPO against mammalian cells, the MTT assay was performed using L929 murine fibroblasts. As fibroblasts are one of the most abundant cells in the skin, low cytotoxic effects on fibroblasts are an essential property of therapeutics for treating infected wounds. Both PO and GPO exhibited no significant cytotoxic effects against L929 cells up to 6.25 mg/mL (Fig. 4). As PEG is known to be a superior biocompatible material, PO consisting of PEG did not show toxic effects. The GPO also exhibited lower cytotoxic effects on L929 cells as NO was released in a sustained manner from the GPO. Without controlled release, NO could exhibit cytotoxic effects by producing reactive nitrogen species that disturb cellular membranes and enzyme functions of eukaryotic cells, such as fibroblasts and keratinocytes. Due to the controlled release of NO provided by the PEG matrix, the GPO could be applied without concerns regarding its toxic effects.

In vivo wound healing study

In vivo wound healing promotion by the GPO was investigated in a mouse MRSA-challenged full-thickness wound model. Although the duration of NO release was 24 h, the GPO was applied every 2 days to avoid stress from the frequent anesthesia. As shown in Fig. 5, facilitated wound size reduction was observed in the GPO-treated group but not in the PO-treated and untreated groups. Macroscopic images of the wounds of the PO-treated and untreated groups revealed that they were covered by bacterial biofilms, whereas those of the GPO-treated group showed clean wound surfaces at day 4 and day 10 due to the elimination of MRSA from the wound site (Fig. 5a). As MRSA was eradicated by NO at the wound site, the GPO-treated group showed faster wound size reduction after treatment initiation than the PO-treated and untreated groups (Fig. 5b). In addition to the eradication of MRSA at the wound site, cell proliferation and tissue remodeling processes were also facilitated by NO, resulting in enhanced wound healing. Conversely, the PO and untreated groups exhibited delayed wound healing owing to the continuous inflammation caused by the MRSA infection. For further investigation, wound sites were excised and stained with H&E for histological examination. As shown in Fig. 5c, H&E images of the GPO-treated group exhibited morphology more similar to healthy skin than the other groups. The epidermis, sebaceous glands, and hair follicles were observed in the GPO-treated group, whereas the PO and untreated groups showed a large number of monocytes and granulocytes. As the untreated and PO groups were

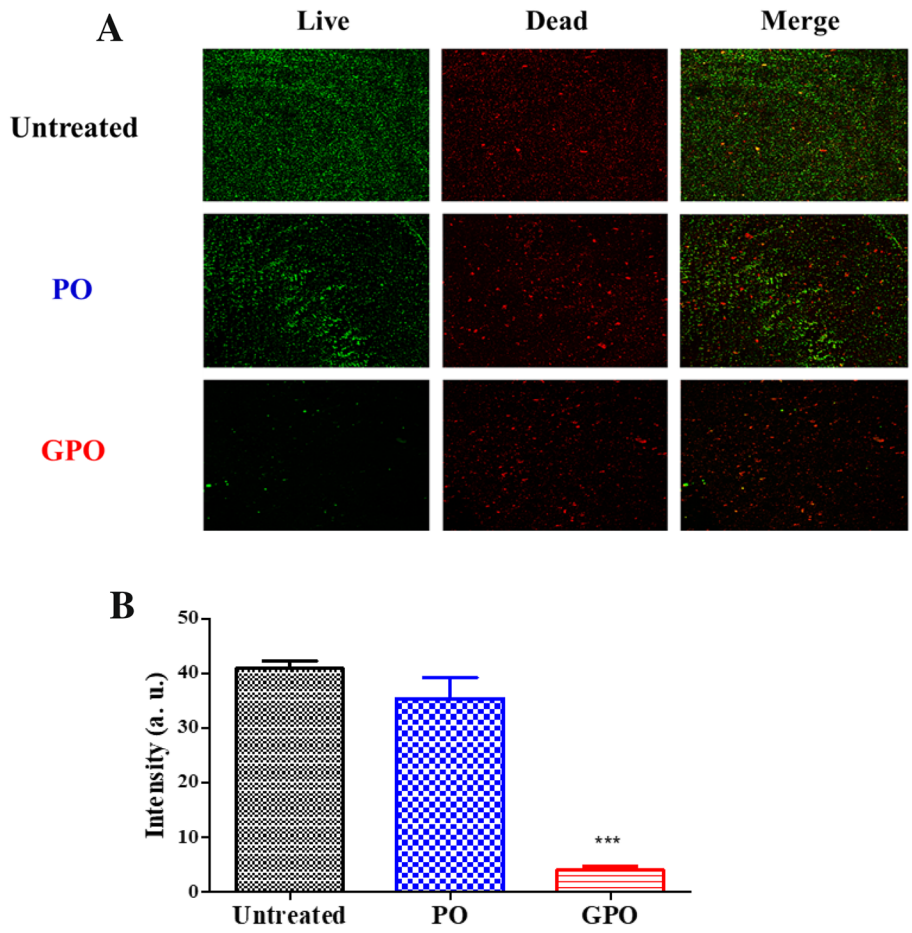

Fig. 3 Antibacterial effect of the GPO against MRSA. **a** Confocal images of MRSA with or without GPO and PO treatment. Green and red fluorescence represent live and dead bacteria, respectively. **b** The intensity of green fluorescence from five different samples in each group. Data are expressed as the mean ± SD

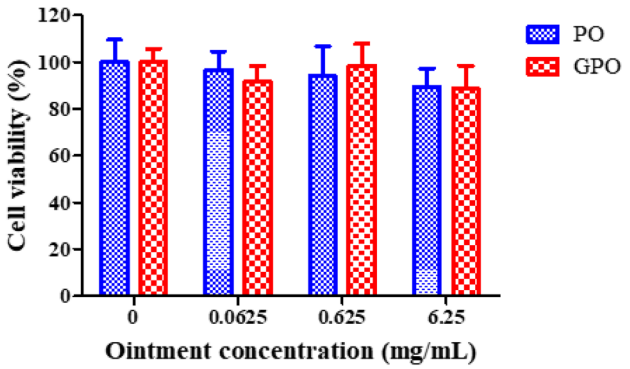

Fig. 4 Cytotoxicity of the GPO and PO in the L929 murine fibroblast cell line using the MTT assay. Data are expressed as the mean ± SD (n = 6)

in an inflammatory phase caused by the MRSA infection, immune cell infiltration remained elevated and tissue restoration was delayed.

Conclusions

In this study, we successfully developed a GSNO-incorporated PEG ointment (GPO) as a novel ointment for the treatment of infected cutaneous wounds. A pink-colored homogeneous GPO was fabricated via micronization of GSNO, dispersion of GSNO into a melted PEG ointment base, and sol–gel transition of the GSNO-PEG suspension by cooling. The GPO released NO in a sustained manner for 24 h without burst release. Significant antibacterial effects of the GPO were observed against MRSA; these results suggested that the GPO possesses potent antibacterial effects. The GPO showed low cytotoxicity up to 6.25 mg/mL towards an L929 murine fibroblast cell line. An in vivo wound healing study using a mouse MRSA challenged full-thickness wound model revealed that the GPO could facilitate infected wound healing by effective eradication of bacteria from the wound and promoting cell proliferation and tissue remodeling. Thus, the GPO could be a promising ointment for the treatment of infected cutaneous wounds.

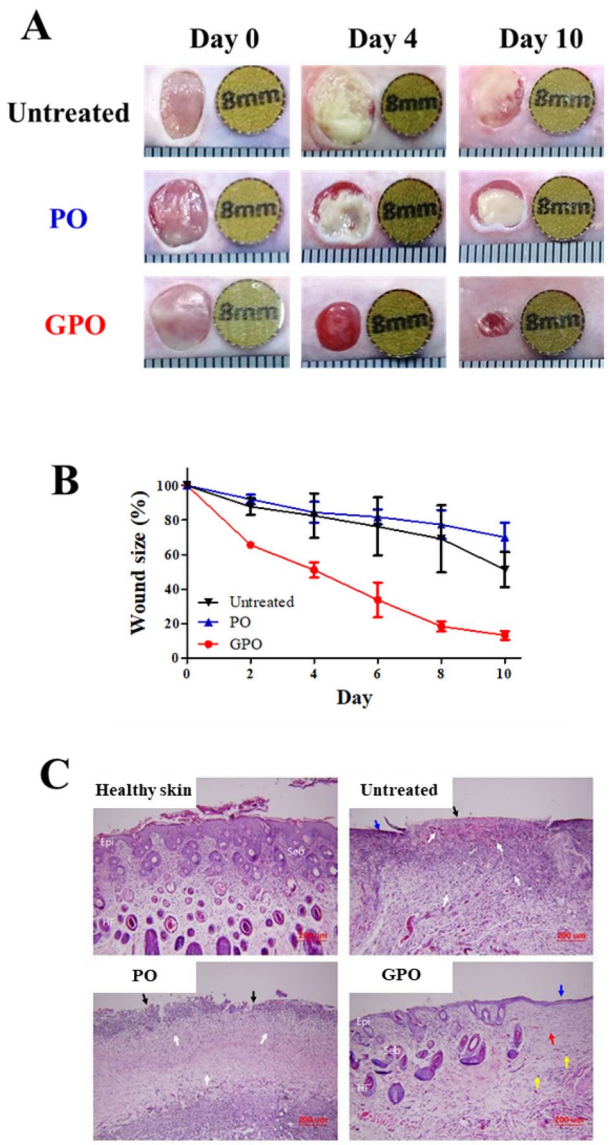

Fig. 5 In vivo wound healing effects of the GPO in a mouse MRSA-challenged full-thickness wound model. **a** Representative macroscopic images of wounds treated with or without GPO. **b** Closure profiles of wounds treated with or without GPO. Values are expressed as the mean ± SD (n = 3). **c** H&E staining of representative wound Sects. 10 days post-treatment. Black, blue, white, yellow, and red arrows indicate ulceration, early epithelium, granulocytes, fibroblasts, and collagen, respectively. *Epi* epidermis, *Seb* sebaceous glands, *HF* hair follicle

Acknowledgements This work was supported by a 2-year research grant from Pusan National University.

Compliance with ethical standards

Conflicts of interest The authors declare that they have no conflict of interest.

Human and animal rights All animal experiments were reviewed and approved by the Pusan National University Institutional Animal Care and Use Committee (PNU-IACUC) on 01 February 2018 (PNU-2018-1800).

References

Amadeu TP, Seabra AB, De Oliveira MG, Costa AM (2007) S-nitrosoglutathione-containing hydrogel accelerates rat cutaneous wound repair. J Eur Acad Dermatol Venereol 21:629–637

Bello YM, Phillips TJ (2000) Recent advances in wound healing. JAMA 283:716–718

Bogdan C (2001) Nitric oxide and the immune response. Nat Immunol 2:907–916

Broniowska KA, Diers AR, Hogg N (2013) S-nitrosoglutathione. Biochim Biophys Acta (BBA) 1830:3173–3181

Choi M, Hasan N, Cao J, Lee J, Hlaing SP, Yoo J-W (2019) Chitosan-based nitric oxide-releasing dressing for anti-biofilm and in vivo healing activities in MRSA biofilm-infected wounds. Int J Biol Macromol 142:680–692

Daeschlein G (2013) Antimicrobial and antiseptic strategies in wound management. Int Wound J 10:9–14

Fleischmann C et al (2016) Assessment of global incidence and mortality of hospital-treated sepsis. Current estimates and limitations. Am J Respir Crit Care Med 193:259–272

Georgii J, Amadeu T, Seabra A, de Oliveira M, Monte-Alto-Costa A (2011) Topical S-nitrosoglutathione-releasing hydrogel improves healing of rat ischaemic wounds. J Tissue Eng Regen Med 5:612–619

Hasan N et al (2019a) Bacteria-targeted clindamycin loaded polymeric nanoparticles: effect of surface charge on nanoparticle adhesion to MRSA. Antibact Activity Wound Heal Pharm 11:236

Hasan N et al (2019b) PEI/NONOates-doped PLGA nanoparticles for eradicating methicillin-resistant *Staphylococcus aureus* biofilm in diabetic wounds via binding to the biofilm matrix. Mater Sci Eng C 103:109741

Hlaing SP et al (2018) S-nitrosoglutathione loaded poly (lactic-co-glycolic acid) microparticles for prolonged nitric oxide release and enhanced healing of methicillin-resistant Staphylococcus aureus-infected wounds. Eur J Pharm Biopharm 132:94–102

Homsy CA (1970) Bio-compatibility in selection of materials for implantation. J Biomed Mater Res 4:341–356

Hornyák I, Pankotai E, Kiss L, Lacza Z (2011) Current developments in the therapeutic potential of S-nitrosoglutathione, an endogenous NO-donor molecule. Curr Pharm Biotechnol 12:1368–1374

Jones ML, Ganopolsky JG, Labbé A, Wahl C, Prakash S (2010) Antimicrobial properties of nitric oxide and its application in antimicrobial formulations and medical devices. Appl Microbiol Biotechnol 88:401–407

Kim JO et al (2015) Nitric oxide-releasing chitosan film for enhanced antibacterial and in vivo wound-healing efficacy. Int J Biol Macromol 79:217–225. https://doi.org/10.1016/j.ijbiomac.2015.04.073

Lee J, Hlaing SP, Cao J, Hasan N, Ahn H-J, Song K-W, Yoo J-W (2019) In situ hydrogel-forming/nitric oxide-releasing wound dressing for enhanced antibacterial activity and healing in mice with infected wounds. Pharmaceutics 11:496

Lin S-Y, Chen K-S, Run-Chu L (2001) Design and evaluation of drug-loaded wound dressing having thermoresponsive, adhesive, absorptive and easy peeling properties. Biomaterials 22:2999–3004

Nurhasni H, Cao J, Choi M, Kim I, Lee BL, Jung Y, Yoo J-W (2015) Nitric oxide-releasing poly (lactic-co-glycolic acid)-polyethylenimine nanoparticles for prolonged nitric oxide release,

antibacterial efficacy, and in vivo wound healing activity. Int J Nanomed 10:3065
Parent M, Dahboul F, Schneider R, Clarot I, Maincent P, Leroy P, Boudier A (2013) A complete physicochemical identity card of S-nitrosoglutathione. Curr Pharm Anal 9:31–42
Privett BJ, Broadnax AD, Bauman SJ, Riccio DA, Schoenfisch MH (2012) Examination of bacterial resistance to exogenous nitric oxide. Nitric Oxide 26:169–173
Rosen J, Landriscina A, Nosanchuk JD (2016) Nitric oxide-releasing nanoparticles as an antimicrobial therapeutic. In: Hamblin MR, Avci P, Prow TW (eds) Nanoscience in dermatology. Elsevier, New York, pp 127–134
Schäffer MR, Tantry U, Gross SS, Wasserkrug HL, Barbul A (1996) Nitric oxide regulates wound healing. J Surg Res 63:237–240
Schairer DO, Chouake JS, Nosanchuk JD, Friedman AJ (2012) The potential of nitric oxide releasing therapies as antimicrobial agents. Virulence 3:271–279
Schanuel FS, Santos KSR, Monte-Alto-Costa A, de Oliveira MG (2015) Combined nitric oxide-releasing poly (vinyl alcohol) film/F127 hydrogel for accelerating wound healing. Colloids Surf B 130:182–191
Stratton CW (2003) Dead bugs don't mutate: susceptibility issues in the emergence of bacterial resistance. Emerg Infect Dis 9:10–16
Wallace JL (2005) Nitric oxide as a regulator of inflammatory processes. Mem Inst Oswaldo Cruz 100:5–9
Witte MB, Barbul A (1997) General principles of wound healing. Surg Clin North Am 77:509–528
Yoo JW, Acharya G, Lee CH (2009) vivo evaluation of vaginal films for mucosal delivery of nitric oxide. Biomaterials 30:3978–3985. https://doi.org/10.1016/j.biomaterials.2009.04.004
Yurt RW, McManus AT, Mason AD, Pruitt BA (1984) Increased susceptibility to infection related to extent of burn injury. Arch Surg 119:183–188